electronic reprint

Journal of
Applied Crystallography
ISSN 0021-8898

First results from a macromolecular crystallography system with a polycapillary collimating optic and a microfocus X-ray generator

Mikhail Gubarev, Ewa Ciszak, Igor Ponomarev, Walter Gibson and Marshall Joy

Journal of
Applied Crystallography
ISSN 0021-8898

Received 7 September 1999
Accepted 2 February 2000

First results from a macromolecular crystallography system with a polycapillary collimating optic and a microfocus X-ray generator

Mikhail Gubarev,[a,b] Ewa Ciszak,[b,c] Igor Ponomarev,[d] Walter Gibson[e] and Marshall Joy[b]*

[a]National Research Council, USA, [b]NASA/Marshall Space Flight Center, Huntsville, AL 35812, USA, [c]Universities Space Research Association, 4950 Corporate Drive, Huntsville, AL 35805, USA, [d]X-ray Optical Systems, Inc., 30 Corporate Circle, Albany, NY 12203, USA, and [e]Center for X-ray Optics, University at Albany (SUNY), NY 12222, USA. Correspondence e-mail: marshall.joy@msfc.nasa.gov

The design and performance of a high-flux X-ray crystallography system, optimized for diffraction measurements from small macromolecular crystals, is described. This system combines a microfocus X-ray generator [40 μm full width at half-maximum (FWHM) spot size at a power level of 40 W] and a short focal length (F = 2.6 mm) polycapillary collimating optic, and produces a small-diameter quasi-parallel X-ray beam. Measurements of the X-ray flux, divergence and spectral purity of the resulting X-ray beam are presented. The X-ray flux through an aperture of 250 μm diameter produced by the microfocus system is 16 times higher than that from a 3.15 kW rotating-anode generator equipped with a pyrolytic graphite monochromator. Diffraction data from lysozyme test crystals collected with the microfocus X-ray system are of high quality and can be reduced with standard crystallographic software, yielding an overall merging factor $R_{\rm sym} \leq 6\%$. Significant additional improvements in flux are possible, and plans for achieving these goals are discussed.

1. Introduction

The ideal X-ray beam for macromolecular crystallography would deliver high flux into an area equal to or slightly larger than that of the sample, be nearly parallel and monochromatic, and be stable and reliable. Synchrotron X-ray sources fulfill all of these requirements for collection of diffraction data from small crystals: the flux of the X-rays channeled into crystals is at least a hundred times higher than that from the best laboratory source. The success of the synchrotron beamlines, however, has not reduced the need for high-brightness X-ray sources in crystal-growth laboratories to perform rapid evaluation of nascent crystals in order to optimize crystal-growth conditions.

High-power X-ray sources such as rotating-anode systems are widely used for laboratory macromolecular crystallography. To form an X-ray beam with the necessary angular divergence and cross section, X-rays from such a source can be collimated by a small pinhole, which transmits a very small fraction of the emitted radiation. Alternatively, focusing or collimating X-ray optics can redirect the X-rays into a useful beam with the necessary angular divergence (Arndt *et al.*, 1998; Owens *et al.*, 1996). Another alternative, which we explore here, is the use of a polycapillary optic (Kumakhov & Komarov, 1990; Li & Bi, 1998) to concentrate the X-ray flux from a microfocus X-ray source onto small crystalline samples. X-rays can be transported through straight or curved capillaries by the use of multiple reflections from the interior of the hollow capillary. Thousands of capillary channels can be combined to form a monolithic optic (Ullrich *et al.*, 1994) and can collect X-rays over a wide solid angle and concentrate them onto the sample (Fig. 1).

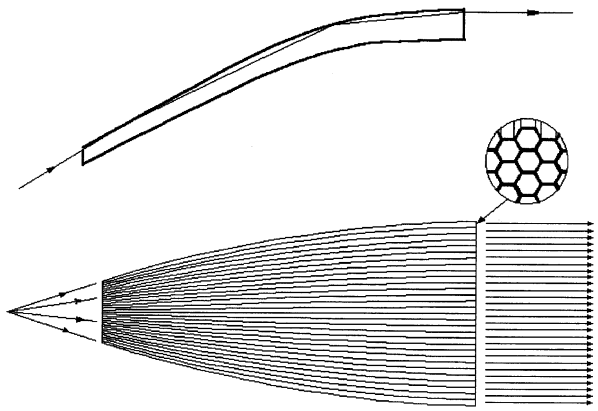

Figure 1
Polycapillary X-ray optics. The X-rays can be guided along straight and curved hollow glass tubes by multiple reflections. The arrays of the polycapillaries can efficiently capture and shape X-ray beams. The cross section of a polycapillary optic is shown schematically in the circular inset.

We have combined a monolithic capillary collimating optic with a new microfocus X-ray generator to produce a laboratory-based X-ray crystallography system. In §2 we present our characterization measurements of the microfocus X-ray source; the characterization of the integrated system is described in §3. §4 compares the performance of the new system with that of a Rigaku rotating-anode generator with a graphite monochromator, and crystallographic results from the new microfocus system are presented in §5. These first results and prospects for future improvements are summarized in §6.

2. Microfocus X-ray source

Two conditions must be met in order to concentrate X-rays efficiently into a tightly collimated intense beam that is useful for protein crystallography. First, the optic must channel the X-rays into a small-diameter collimated beam that is comparable to the size of the samples to be studied (less than 0.5 mm for most crystals). Second, the optic must capture a substantial fraction of the solid angle emitted by the X-ray source in order to deliver the highest flux. These requirements place stringent constraints on the X-ray generator. The optic must be located extremely close to the X-ray source in order to collect photons over a significant solid angle, and the X-ray spot size must be very small in order to feed the collimating optic efficiently.

In our experiments, we used an UltraBright microfocus X-ray source with a copper anode, manufactured by Oxford Instruments, Inc. (http://www.oxinst.com/xtg/pdfs/ubflyer.pdf). The UltraBright source consists of a power supply integrated with a sealed X-ray tube, and an external controller. This source is designed so that the electron beam is focused very close to the X-ray output window. The controller allows for adjustment of the electron focusing system, so that it is possible to vary the X-ray spot size.

Our characterization of the microfocus X-ray source consisted of the following measurements: Cu $K\alpha$ X-ray flux as a function of high voltage, the distance between the anode spot and the output window, the spatial stability of the anode spot, and the spot size as a function of tube voltage and current.

2.1. Cu $K\alpha$ flux as a function of applied voltage

To optimize the operating parameters of the source, the Cu $K\alpha$ (8.04 keV) X-ray flux was measured as a function of high voltage. For this measurement, an Amptek (http://www.amptek.com/xr100czt.html) CdZnTe detector with a 300 μm pinhole was placed 50 cm from the source. The beam current was 8 μA. We found that the Cu $K\alpha$ X-ray flux increases linearly as a function of high voltage up to 45 kV and then becomes constant; therefore, an operating voltage of 45 kV was selected for the remaining measurements.

2.2. Distance between X-ray spot and output window

The distance between the outside surface of the beryllium window and the anode spot was measured to determine how close the collimating optic could possibly get to the X-ray spot. The UltraBright source was installed on an *XY* stage and a 10 μm pinhole, made in gold foil, was placed 33.1 mm from the output window of the source (distance c in Fig. 2). Pinhole images of the anode spot were recorded on polaroid film installed 205 mm from the pinhole (distance d in Fig. 2). The spot–window distance was calculated from the change in position of the pinhole image on the film with respect to the change in source position (Fig. 2). The distance between the outside surface of the beryllium window and the anode spot was measured at several voltage settings and was found to be 1.8 (1) mm.

2.3. Optimization of the X-ray spot size

The acceptance cone of the polycapillary optic should be matched as closely as possible to the size of the anode spot. To measure the spot size and to find the optimum focus settings, we used the X-ray pinhole imaging setup and recorded images of the anode spot on high-resolution Kodak TekPan X-ray film, which was then scanned with a microdensitometer. The X-ray spot image obtained at 45 kV tube voltage and 0.45 mA current (20 W power) is shown in Fig. 3. The image of the anode spot is nearly circular at all power settings. The minimum FWHM spot sizes for different power settings (with a constant tube voltage of 45 kV) are shown in Table 1.

2.4. Stability of the X-ray spot

Since the polycapillary optic captures the X-ray photons from a limited acceptance cone, even a small drift in the spot position can result in a significant decrease in the X-ray output. We used the same experimental setup (with an Amptek CdZnTe detector in the place of film) to measure the positional stability of the X-ray spot. At a fixed voltage and

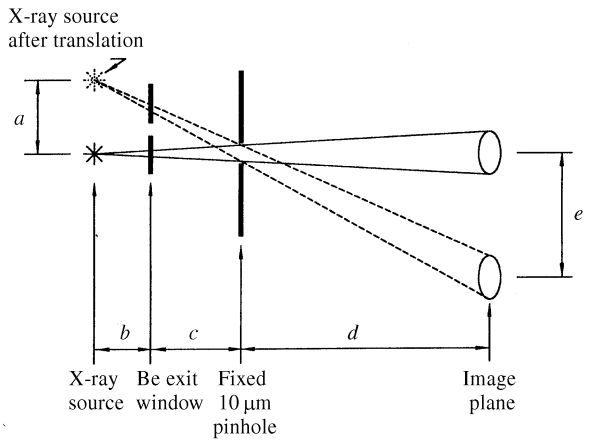

Figure 2
The source–window distance (b) can be calculated from the change in position of the pinhole image (e) with respect to the change in source position (a). The distances between the source, the pinhole and the image plane (c, d) are fixed. By triangulation, the source-to-window distance is related to the other related parameters by $b = ad/e - c$.

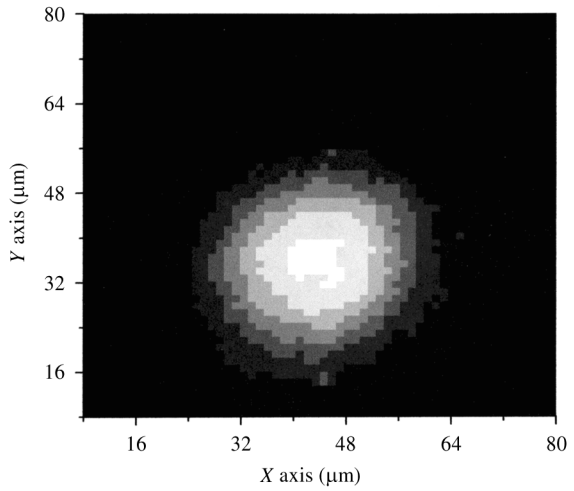

Figure 3
Pinhole image of the anode spot recorded at 45 kV tube voltage and 0.45 mA current. Dimensions are scaled to the actual size of the anode spot.

current we did not detect any measurable drift of the centroid of the X-ray spot over a period of 16 h; the accuracy of this measurement is estimated to be ± 2 μm. [We noted that significant displacement of the X-ray spot was observed when the high voltage or current were changed; for example, the X-ray spot centroid moved 45 (5) μm when the tube voltage was changed from 20 kV to 40 kV at a fixed beam current of 100 μA.]

3. Characterization of the microfocus X-ray crystallography system

3.1. Polycapillary collimating optic

In our experiments we used a polycapillary X-ray collimating optic manufactured by X-ray Optical Systems, Inc. (http://www.xos.com). This optic is designed to capture efficiently X-rays emitted from the microfocus X-ray source and collimate them into a small-diameter quasi-parallel X-ray beam. The specifications of the polycapillary X-ray collimator are listed in Table 2. The transmission efficiency was measured using a low-power X-ray source (a modified 'International Scientific Instruments' scanning electron microscope) with a 18 μm FWHM X-ray spot size. For this measurement, a pinhole of 0.5 mm diameter was placed at the output of the polycapillary collimator, so the linear capture angle was about 0.1 rad.

To integrate the polycapillary collimator into the microfocus system, the optic was installed on an *XY* stage and the input of the optic was placed 2.6 mm from the UltraBright X-ray source. In order to align the optic with respect to the anode spot, this assembly was also placed on a translation stage so that the distance between the input of the optic and the X-ray source could be adjusted. The Amptek CdZnTe detector was installed 140 mm from the output of the polycapillary collimator. The X-ray optic was aligned with respect to the X-ray source by maximizing the Cu $K\alpha$ count rate at the detector.

Table 1
Minimum X-ray spot size for different power settings measured at 45 kV tube voltage.

Power (W)	10	20	30	40
Minimum X-ray spot size (FWHM) (μm)	28 (2)	30 (2)	37 (2)	41 (2)

Table 2
Specifications of the polycapillary X-ray collimator.

Transmission efficiency for 8.04 keV X-rays (%)	41 (2)
Input diameter (mm)	0.91
Output diameter (mm)	1.8
Focal distance (mm)	2.6
Length (mm)	10.14

3.2. X-ray flux measurements

To measure the X-ray flux produced by the polycapillary collimator, a 250 μm pinhole made in lead sheet of 1 mm thickness was installed after the optic. The pinhole was aligned with the X-ray beam. In order to prevent saturation of the Amptek CdZnTe detector, an attenuator consisting of 250 μm nickel and 125 μm titanium foils was placed between the optic and the detector. Prior to installation, the attenuation was measured as a function of X-ray energy and the measured attenuation factors were applied to the raw count rates to determine the true Cu $K\alpha$ flux. The measurements were made at power level of 40 W (897 μA tube current and 45 kV tube voltage). The Cu $K\alpha$ count rate produced by the polycapillary optic with a 250 μm pinhole and a 10 μm nickel filter was $1.20\ (15) \times 10^7$ counts s^{-1} at a power level of 40 W. A similar measurement was made with a 10 μm nickel filter inserted at the output of the optic to monochromatize the beam. The total X-ray flux through the 250 μm pinhole and the 10 μm nickel filter was $1.40\ (15) \times 10^7$ counts s^{-1}, indicating that 86 (2)% of the photons produced by the system are with the Cu $K\alpha$ lines.

3.3. Profile of the X-ray beam

To measure the cross-sectional profile of the output X-ray beam, the detector was placed on a four-axis stage with two spatial and two rotational degrees of freedom (X, Y, θ_x, θ_y). A 25 μm pinhole made in lead sheet of 1 mm thickness was installed on the detector. The pinhole was aligned with respect to the X-ray beam by maximizing the X-ray flux through the pinhole. The detector and pinhole then scanned through the X-ray beam in the vertical and horizontal directions. The two profiles are nearly identical, and the size of the beam is 480 (20) μm FWHM (Fig. 4). Integration of these profiles over a central area of diameter 250 μm can be used to determine the X-ray flux independently, and is in good agreement with the X-ray flux measured using a 250 μm pinhole, described in §3.2.

3.4. Beam divergence

To measure the divergence of the beam, a 250 μm pinhole was installed after the polycapillary collimator and aligned with respect to the beam. High-resolution Kodak TekPan X-

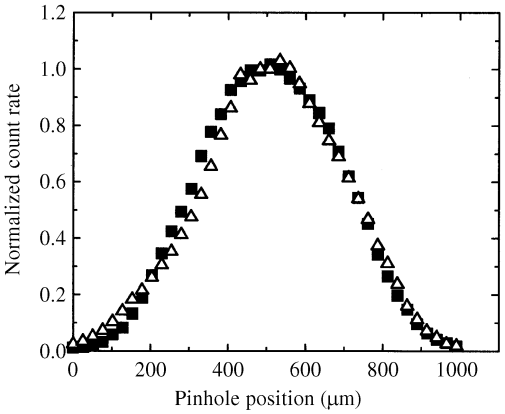

Figure 4
Profile of the X-ray beam produced by the polycapillary X-ray optic, measured at 8.04 keV (Cu $K\alpha$ line). The horizontal scan is shown with solid squares, and the vertical scan with open triangles. The scans were made at a distance of 140 mm from the output of the polycapillary collimator.

ray film was placed 120 mm from the pinhole. The divergence was calculated from the relative size of the X-ray image and the pinhole diameter, and was found to be 0.25 (2)° FWHM.

4. Characterization of a standard rotating-anode X-ray crystallography system

We used a Rigaku RU-200 rotating-anode X-ray crystallography system as a benchmark against which the X-ray microfocus system could be compared. The X-ray beam from the rotating-anode source is collimated by a pyrolytic graphite monochromator and a 250 μm pinhole collimator.

4.1. X-ray flux measurements

To measure the X-ray flux from the Rigaku X-ray system, the Amptek CdZnTe detector was placed on a four-axis stage. The input window of the detector was installed 350 mm from the pinhole collimator of the X-ray source. In order to prevent the saturation of the detector, a 125 μm nickel foil was installed between the X-ray source and the detector. Prior to installation, the attenuation of this nickel foil was measured as a function of the X-ray energy, and the attenuation factors were applied to the raw count rates to determine the true Cu $K\alpha$ flux. The Cu $K\alpha$ count rate produced by the Rigaku X-ray system was measured to be 7.5 (2) $\times 10^5$ counts s^{-1} at 3.15 kW power (45 kV voltage and 70 mA current). We compare this result with that obtained from the microfocus X-ray crystallography system in §6.

4.2. Profile of the X-ray beam

For this measurement, a 50 μm pinhole made from lead sheet of thickness 1 mm was placed on the detector. The pinhole was aligned with respect to the X-ray beam by maximizing the X-ray flux through the pinhole. The profile of the beam was scanned in the vertical and horizontal directions. The size of the beam is 970 (50) μm and 590 (50) μm FWHM in the horizontal and vertical directions, respectively (Fig. 5).

4.3. Beam divergence

For this measurement we used a three-axis (ω, φ, 2θ) goniometer with a Bruker HI-STAR detector installed on the 2θ goniometer arm. A silicon crystal was installed on the rotating goniometer head. The beam divergence measured in the horizontal direction was 0.14 (1)° FWHM (Fig. 6).

5. Diffraction data from the microfocus system

To evaluate the quality of crystallographic data produced by the microfocus X-ray system, several diffraction data sets using crystals of the tetragonal form of lysozyme (chicken egg white) were measured and processed. The data were collected at room temperature. A schematic drawing of the diffraction experiment is shown in Fig. 7. The microfocus X-ray source

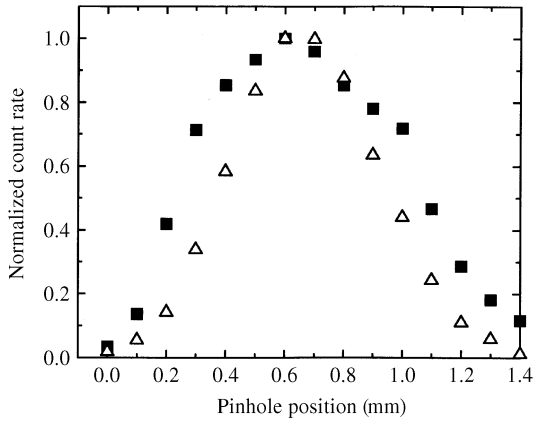

Figure 5
Profile of the X-ray beam produced by the rotating-anode X-ray source, measured at 8.04 keV (Cu $K\alpha$ line). The horizontal scan is shown with solid squares, and the vertical scan with open triangles. The scans were made at a distance of 350 mm from the pinhole collimator of diameter 250 μm.

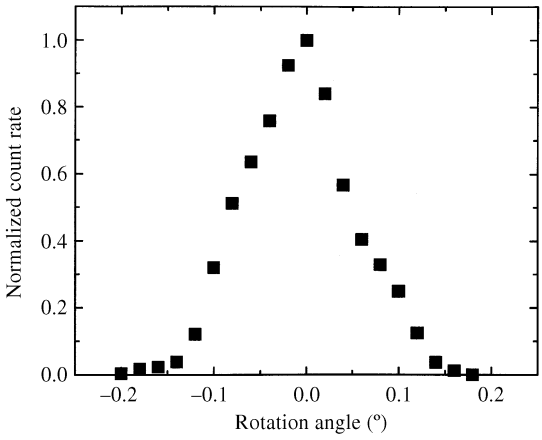

Figure 6
Angular profile of the X-ray beam produced by the rotating-anode source measured in the horizontal direction.

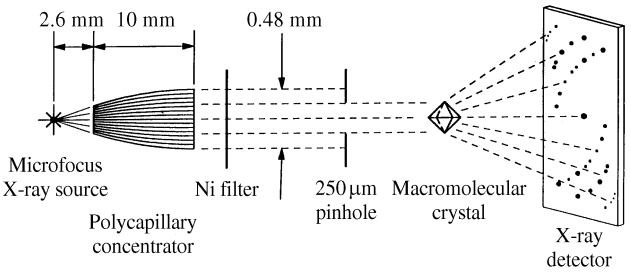

Figure 7
Schematic representation of the macromolecular crystallography system.

was operated at 40 W (45 kV and 897 μA) and the X-ray radiation was filtered with a 10 μm nickel foil. The X-ray beam was collimated by a 250 μm pinhole. The optic-to-crystal distance was 6 cm. In each case, lysozyme crystals were mounted on a Siemens three-axis goniometer and data were recorded using a HI-STAR multiwire detector. The data collection was controlled by *FRAMBO* V.3.003 and the raw frames were processed with *SAINT* V.5 on a Silicon Graphics workstation (Bruker X-ray Analytical Systems, 1995). The longest dimension of the lysozyme crystals used for the experiments was $\leq$0.20 mm.

We have collected several complete diffraction data sets that resulted in similar data processing statistics. In each case the complete sets of diffraction data was collected in ω and φ scans with an oscillation angle of 0.25° over a period of several hours. Several crystals diffracted up to 1.7 Å resolution with gradually increasing signal-to-background ratio. We chose to consider diffraction data as significant if at least half of the reflections in the outermost resolution shell of 0.1 Å thickness

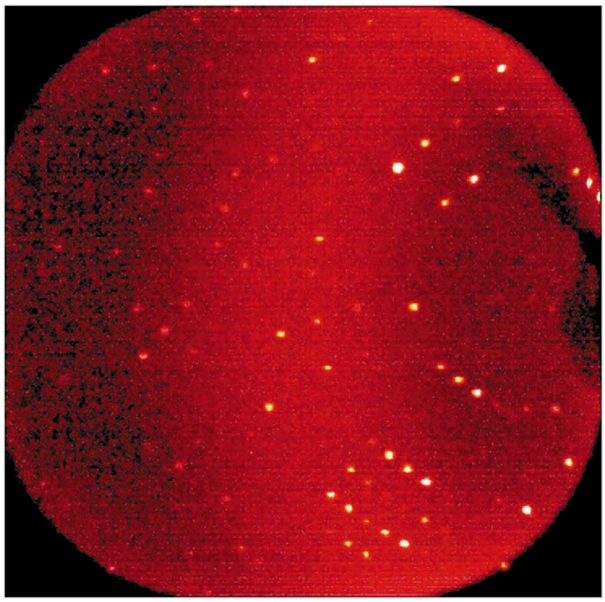

Figure 8
A single diffraction image from a lysozyme crystal recorded on a HI-STAR multiwire detector using the microfocus X-ray system. The crystal is tetragonal, with cell dimensions $a = b = 79.12$, $c = 38.40$ Å. The data were collected at a swing angle of 25° and a crystal-to-detector distance of 11.8 cm, with a maximum recorded resolution of 1.98 Å.

Table 3
Data collection conditions.

Crystal size (mm)	0.15 × 0.18 × 0.18
System, space group	Tetragonal, $P4_32_12$
Unit cell parameters (Å)	$a = b = 79.12$, $c = 38.40$
Collimator diameter (mm)	0.25
Crystal-to-detector distance (cm)	11.86
Frame width (°)	0.25
Exposure time (s)	120
Detector diameter (mm)	100
Swing (2θ) angle (°)	25
Number of frames	362

Table 4
Summary statistics for ten resolution shells.

Shell (Å)	Completeness (%)	Redundancy	Cumulative R_{sym} (%)	R_{sym} in resolution shells (%)	Average I/σ
To 4.288	88.72	2.90	4.8	4.8	39.98
To 3.412	92.39	2.81	5.1	5.4	24.61
To 2.983	93.69	2.68	5.2	6.2	12.00
To 2.712	94.10	2.54	5.4	7.4	6.81
To 2.518	93.95	2.44	5.5	8.9	5.08
To 2.370	93.29	2.36	5.7	9.9	3.95
To 2.252	92.30	2.30	5.8	11.2	3.42
To 2.154	90.80	2.25	5.9	13.6	2.60
To 2.071	89.10	2.20	6.0	15.7	2.23
To 2.000	86.60	2.15	6.0	17.5	1.78

were significantly above the background with $I \geq 2\sigma(I)$. Fig. 8 shows an example of a single oscillation image from the experiment summarized in Table 3. 16 273 observations yielded 7650 unique observations extending to 2.0 Å resolution. The merging R factor computed from the integrated intensity, I, of the reflection, and the mean, $\langle I \rangle$, of all observations of the reflection and its symmetry equivalents ($R_{sym} = |I - \langle I \rangle|/|\langle I \rangle|$) is 6.02%. The summary statistics for resolution shells are shown in Table 4.

The diffraction data collected with our microfocus X-ray source and collimating polycapillary are of good quality. The resolution and the average intensity of reflections and their signal-to-background ratio represented in a statistical manner have demonstrated the capability of the microfocus system for X-ray crystallography, including macromolecular crystallography, and have encouraged us to improve the prototype system further.

6. Conclusions

We have presented the first results from a microfocus X-ray source coupled with a polycapillary collimating optic, which produces a small-diameter quasi-parallel X-ray beam for macromolecular crystallography. The Cu $K\alpha$ X-ray flux produced by the microfocus system is 16 times higher than that from a standard rotating-anode generator equipped with a graphite monochromator. Remarkably, this high flux was produced by a source that uses 78 times less power than the rotating-anode generator. Diffraction data collected with the microfocus X-ray system are of high quality and can be reduced with standard crystallographic software; for example,

the diffraction data from a test lysozyme crystal yielded an overall merging factor R_{sym} = 6.02% at 2.0 Å resolution.

Although these results are dramatic, it is possible to achieve significantly higher X-ray intensity without loss of quality of diffraction data by using an optic that produces a weakly convergent beam. This will allow X-rays from an even larger collection angle to be incident on small crystals; a flux gain of an additional order of magnitude is anticipated.

In a subsequent paper, we will report on measurements made with a weakly convergent polycapillary optic, and will compare the results with the performance of an advanced rotating-anode system with multilayer concentrating optics.

We thank Marcus Vlasse for providing the goniometer and detector used for the crystallographic measurements, and Jeff Kolodziejczak and Walter Fountain for assistance with microfocus source characterization.

References

Arndt, U. W., Long, J. V. P. & Duncumb, P. (1998). *J. Appl. Cryst.* **31**, 936–944.

Bruker X-ray Analytical Systems (1995). *SMART Program Package* V.5. Bruker X-ray Analytical Systems, Inc., Madison, Wisconsin, USA.

Kumakhov, M. A. & Komarov, F. F. (1990). *Phys. Rep.* **191**, 289–350.

Li, P.-W. & Bi, R.-Ch. (1998). *J. Appl. Cryst.* **31**, 806–811.

Owens, S. M., Ullrich, J. B., Ponomarev, I. Yu., Carter D. C., Sisk, R. C., Ho, J. C. & Gibson, W. M. (1996). *Proc. SPIE*, **2859**, 200–209.

Ullrich, J. B., Ponomarev, I. Yu., Gubarev, M. V., Gao, N., Xiao, Q. F. & Gibson, W. M. (1994). *Proc. SPIE*, **2278**, 148–154.